UNIVERSITY OF WEST ATTICA

eISSN:3136-7658

Applied Manufacturing Intelligence Journal

Vol. 5, No. 1, January, 2026



Edge-Aware CausalTFT Model for PCB Solder Bridging Segmentation

Poyraz Korkmaz[a,*], Davut Gür[a], Ferhat İnan[a]

[a] *Faculty of Electrical and Electronics Engineering, Istanbul Technical University, Istanbul, 34469, Turkey*

Received 27 October 2025; Revised 19 January 2026; Accepted 22 January 2026; Published 28 January 2026

Abstract

Solder bridging is a serious assembly defect in printed circuit board manufacturing because a small conductive connection between adjacent pads can cause electrical failure, rework and long-term reliability risk. This paper introduces an edge-aware CausalTFT model for PCB solder bridging segmentation in optical inspection. The method constructs an image window from pad-edge response, solder-region intensity, local continuity, component layout and image-quality indicators. Edge-aware representation improves the boundary separation among solder, pad and substrate, while a causal temporal fusion transformer backbone combines spatial evidence, short production-window context and source reliability. A causal gating branch reduces unstable correlations caused by reflection, flux residue, shadow, solder-mask colour variation and partial occlusion. The simulated dataset contains normal joints, weak bridges, severe bridges, reflection artefacts and paste-overflow cases. Experimental results show that mean intersection over union reaches 94.2%, bridge recall reaches 92.8% and boundary F1 reaches 89.6%, outperforming ordinary UNet, DeepLab-style and Transformer baselines. Confidence outputs and dominant-evidence records are used to separate true solder bridges from uncertain bright regions. For high-mix PCB assembly, the output also preserves pad-gap geometry, inspection-window reliability and package-level context so that review personnel can distinguish conductive bridge risk from imaging disturbance. The framework supports bridge mask prediction, bridge probability estimation, evidence traceability and review prioritisation for line-side PCB assembly inspection.

Keywords: PCB Solder Bridging Segmentation; Edge-Aware Learning; CausalTFT; Industrial Optical Inspection; Production Review

1. Introduction

Printed circuit board assembly requires stable solder joints because open circuits, insufficient solder and solder bridging can directly influence electronic reliability [1]. Automated optical inspection has become an important production method for detecting visible assembly defects before electrical testing [2]. Solder bridging is especially difficult because the connection between adjacent pads may be narrow, reflective and partly hidden by component geometry [3]. Deep segmentation models have improved defect localisation, but their reliability depends on boundary quality, image contrast and representative production data [4]. In a real line, a bridge mask must not only overlap the bright solder region but also indicate whether the conductive connection crosses the pad gap. This requirement makes solder bridging segmentation different from ordinary bright-object segmentation. A small false-positive area can waste review resources, while a small missed connection can allow a defective board to enter functional testing.

Most inspection systems at present are based on rules and thresholds, templates and learned visual features. Rule-based methods are relatively stable in the condition of uniform light and board type, but their transferability is low when the solder mask colour, pad size or component package changes [5]. Although CNN-based segmentation models can learn local texture and shape features, they may be affected by flux residue, reflection and uneven paste in the real

* Corresponding author: poyraz.kor@itu.edu.tr

https://doi.org/10.68406/amij.2026.vol5iss1np4:42-53

➢ This is an open access article under the CC BY-NC-SA 4.0 license (https://creativecommons.org/licenses/by/4.0/).

© Authors retain all copyrights.

joint [6]. Transformer-based methods can improve the long-range reasoning of non-local parts, but dense attention is still computationally expensive for high-resolution production images [7]. Recent studies of industrial AI have also shown that inspection systems should provide confidence levels and supporting evidence instead of just a binary label [8]. To know whether the model will indicate that the cause of the warning is a pad-edge connection, a solder discontinuity, abnormal brightness, or a weak image, examine the PCB solder bridging.

Therefore, the present study considers solder bridging segmentation a problem in evidence-controlled production. Draw a mask based on the drawing, and at the same time, determine whether there is supporting reliable physical and visual evidence for this mask. The proposed edge-aware CausalTFT model restricts the candidate bridge region by employing a pad-edge response, stabilizes the evidence from neighbouring inspection windows through temporal fusion, and suppresses unstable correlations induced by lighting or surface contamination via causal gating. It will also return the confidence and review priority of each item, and low-confidence samples will be sent for manual inspection instead of being deemed permanently invalid. This Design is suitable for line-side deployment, and high throughput, traceability and false-alarm control are all required.

The research is organised by the modelling problem and engineering verification. Section 2 reviews PCB optical inspection, edge-aware segmentation and causal temporal fusion for production review. Section 3 introduces image evidence representation, the CausalTFT backbone and calibrated output design. Section 4 presents segmentation simulation results, boundary robustness tests, causal evidence analysis and production review output. Section 5 summarizes the main findings, deployment limitations and future validation requirements for PCB assembly inspection.

2. Related Work

2.1. PCB Solder Bridging Inspection

Solder bridge inspection of PCBs generally occurs after paste printing, component placement and reflow. There is a defect; the solder has connected the neighbouring pads or pins by accident. Research on optical inspection has found that the causes of solder defects include changes in paste volume, stencil opening, pad shape, reflow temperature and component misalignment [9]. Due to the above reasons, the following problems have occurred: bright bridges, dull paste overflow, thin residual filaments, and shaded inter-pin connections. A single upper bound for brightness is not suitable in production. The input of the segmentation model should be local intensity, padding context and boundary continuity.

Board-level Differences are also reasons for failure. Fine-pitch integrated circuits, connectors and passive components have different gap sizes and solder shapes. Based on research of assembly inspection, defect interpretation should consider package type and adjacent-pad distance [10]. A small solder bump near a large pad is likely to be harmless, and similarly, a row of fine pins with the same appearance width may be a bridge. Therefore, the model should preserve the layout context and not consider every bright area an individual object. Therefore, edge constraints and region-aware features are employed to tackle this problem.

Another problem is the presence of real bridges and artificial defects. Flux residue, scratches, copper exposure, solder mask variations and specular reflections can all be bright areas that appear as bridges. According to industrial inspection studies, low-confidence alarms need to be verified with supporting evidence [11]. The record of evidence for PCB production should include bridge location, boundary connection, image quality and the primary reason for the warning. Otherwise, the repeated false alarms cannot be linked to changes in camera settings, light angles or process drift.

2.2. Edge-Aware Segmentation Models

Edge-aware segmentation is more suitable for problems that need to locate the boundaries of defects precisely. Solder bridging is the formation of a continuous path across the insulating gap of the conductive pads by solder. Boundary-guided segmentation studies have shown that adding edge cues can improve small-object and thin-structure prediction [12]. A solder bridge needs to be added at a small section of the image. Therefore, the model needs to extend the pad-gap edges and solder contours and then generate the final mask.

Most segmentation networks are encoder-decoder architectures that use feature pyramids and skip connections. First of all, there are still boundary errors in the areas with weak texture or high reflectivity that need to be corrected. Recently, in research on small-defect segmentation, boundary supervision and multi-scale features have improved localisation under class imbalance [13]. There is a significant imbalance in the PCB images; the area of the normal board is relatively large, and the bridge pixels are scarce. A model optimised only by pixel-wise loss will not be able to recognise a faint bridge.

Border information is not to be taken as absolute. Pad edges may be covered by the component body, and solder reflection can change the detected boundary. Research on Robust Segmentation shows that auxiliary edge cues need to

be added with confidence control [14]. Edge Response is used as the evidence in this study and was not chosen in advance. The model can reduce the effect of the edge in areas of blur, shadow or local occlusion. Avoid a false certainty due to unreliable boundary extraction.

2.3. Causal Evidence for Industrial Prediction

Model building for causal evidence helps address the problem of spurious correlations in production images in inspections. The model may have learned that the reflection pattern is related to a defect because most of the defective samples were taken in a certain light. Causal learning studies in visual recognition have shown that it is necessary to distinguish between stable causes and accidental background correlations [15]. The cause of a solder bridge in PCB inspection is a continuous electrical connection across the pads, not a general decrease in image brightness.

Temporal fusion can also support line-side inspection. Although a PCB image is spatially fixed, nearby board windows and adjacent component regions can provide reference information about lighting, camera focus and process conditions. Yan and Xiao [16] showed that temporal-variable Transformer structures with gated fusion can improve the modelling of heterogeneous sequence features. Therefore, the CausalTFT design is suitable for combining image tokens, edge statistics and quality indicators in a controlled manner. It selects evidence according to the current board region and avoids assigning a fixed weight to all features.

Explainable inspection is also necessary for production review and maintenance. Bitterling et al. [17] demonstrated that explainable visual inspection can improve human-centred quality control by linking model outputs with review evidence. For solder bridging segmentation, the useful outputs include bridge mask, bridge probability, confidence, dominant evidence and review priority. These outputs can support line-side decisions and process analysis. If repeated alarms are caused by weak boundary evidence, camera calibration may be required; if the alarm is associated with actual solder discontinuity near a specific package, stencil design or reflow settings should be inspected.

3. Methodology

3.1. Edge-Aware Image Evidence Representation

The input is a production inspection window centred on a PCB pad group. The representation includes solder-region image response, pad-edge response, candidate bridge continuity, component-layout position and image-quality index. Figure 1 shows the edge-aware evidence construction workflow. the optical inspection image, pad edges and solder candidates are extracted, aligned with the pad gap and converted into a segmentation window for CausalTFT processing. This representation follows the physical definition of a bridge because the candidate region must connect conductive structures rather than merely appear as an isolated bright spot.

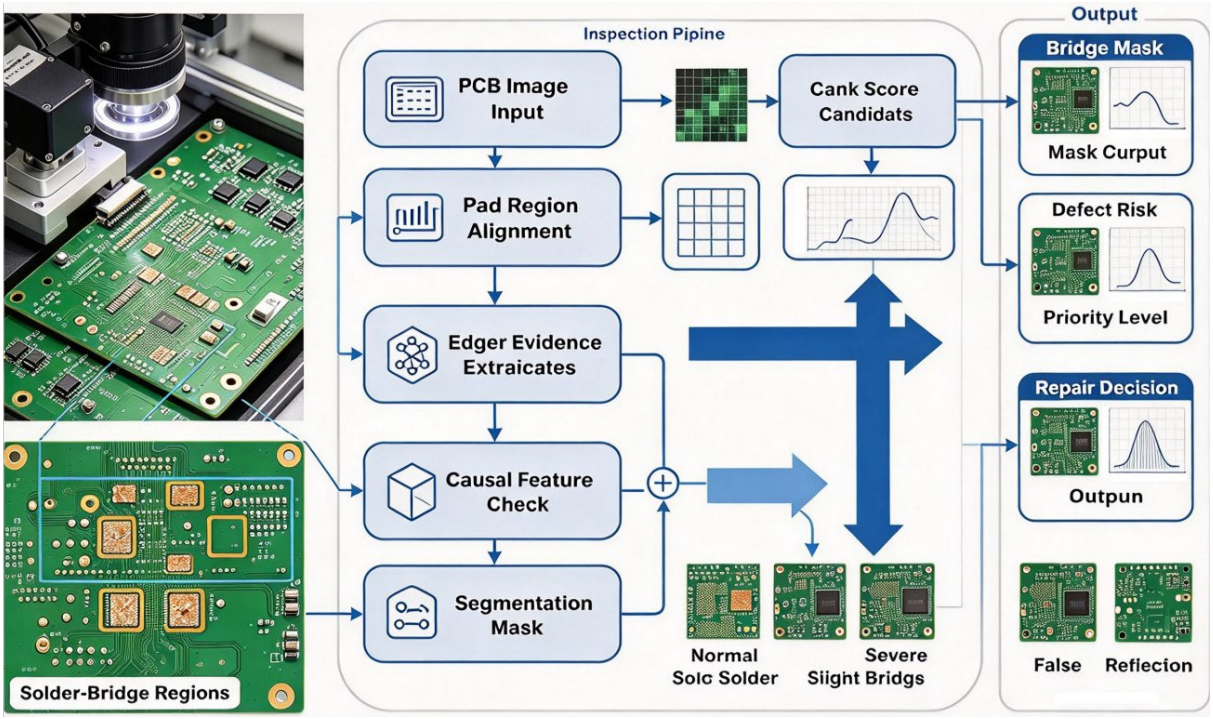


Figure 1. Edge-Aware PCB Solder Bridging Evidence Construction Workflow

The first representation describes the bridge candidate response. It combines solder intensity, local edge support and pad-gap proximity so that isolated bright spots receive less emphasis than connected solder structures.

$$R_t = I_t E_t + \beta G_t \tag{1}$$

The response map is used as a candidate representation before segmentation. It does not determine the final mask because reflection, flux residue and paste overflow can produce similar intensity. The model therefore keeps this response as one source of evidence.

The second representation describes edge-aware bridge weight. The value increases when a candidate region crosses a pad gap with continuous edge support and decreases when the candidate is far from conductive boundaries.

$$B_t = \frac{C_t P_t}{1 + D_t} \tag{2}$$

Weight helps the model distinguish a real inter-pad connection from a local solder bulge. There is also a delay in the explanation, and the warning generated for a high-bridge-weight problem is different from that generated for brightness.

Image quality is also displayed in this window. The components of the quality vector are blur, glare, shadow and occlusion indices. These values are not used to exclude samples from the dataset. The model has given some attention to the evidence in segmentation and confidence calibration. The Quality vector is considered a reliability condition rather than a cause of defects. A low-quality image may still have the original bridge; a high-quality image may contain a false reflection. Alter the weight of confidence and evidence using a quality vector, rather than excluding samples or modifying the ground-truth labels in the model.

3.2. CausalTFT Segmentation Backbone

Figure 2 shows the CausalTFT segmentation backbone. Edge-aware tokens, solder-region tokens and quality indicators are first mapped into a common feature space. The temporal fusion branch learns relations among adjacent inspection windows, and the causal gate adjusts feature contribution according to source reliability. The decoder then outputs the bridge mask and review-related features. the model jointly considers local solder appearance, pad-gap structure, short production context and reliability before producing a segmentation decision.

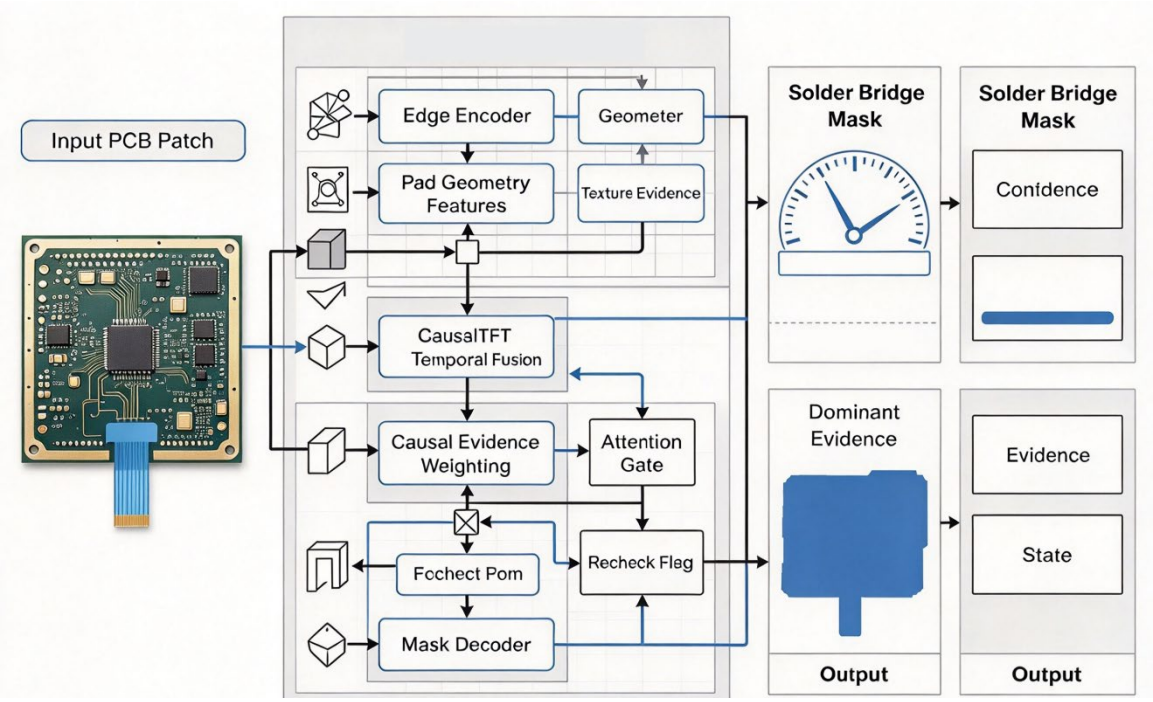


Figure 2. CausalTFT Segmentation Backbone for PCB Solder Bridging

The token embedding stage maps visual and structural evidence into a compact representation. This representation preserves pad-gap location and candidate solder continuity before causal fusion.

$$u_t = W_x x_t + W_r R_t + W_b B_t \tag{3}$$

The fused input token keeps three kinds of information in one state: raw visual appearance, candidate response and edge-aware bridge weight. This avoids a decision based only on bright pixels.

The temporal fusion branch uses a gated update to retain stable production context from neighbouring windows and suppress unstable disturbances.

$$h_t = \phi(W_h h_{t-1} + W_u u_t) \tag{4}$$

The hidden state stores short-range inspection context. It helps the model recognise whether a bright line is an isolated artefact or part of a repeated process pattern across the board region.

The causal gate adjusts feature contribution according to source reliability. A variable with strong statistical response is not automatically trusted if it is linked to poor image quality.

$$g_t = \text{sigmoid}\big(W_g[h_t, q_t]\big) \tag{5}$$

The gated representation is then passed to the segmentation decoder. The decoder combines local boundary information and global pad-gap context to produce the bridge mask.

$$m_t = \text{sigmoid}\big(W_m(g_t * h_t)\big) \tag{6}$$

3.3. Segmentation Loss and Output Calibration

The training objective combines segmentation accuracy, boundary consistency and confidence calibration. It is designed for production inspection because mask overlap alone cannot reflect the cost of missing a conductive bridge.

$$L_s = L_{\text{dice}} + \lambda_b L_{\text{edge}} \tag{7}$$

The segmentation term controls mask overlap and edge localisation. Boundary consistency is included because a small shift across the pad gap can change the engineering meaning of the predicted mask.

The final objective adds causal regularisation and confidence calibration. The causal term suppresses unstable evidence, and the calibration term aligns confidence with actual prediction reliability.

$$L = L_s + \lambda_c L_{\text{causal}} + \lambda_u L_{\text{cal}} \tag{8}$$

The final result includes bridge mask, bridge probability, confidence, dominant evidence and review priority. A high-confidence bridge can trigger rejection or repair, whereas a low-confidence candidate should be sent for secondary inspection. The output design does not treat all bright areas as production risks. Review priority is determined after evaluating mask geometry, pad-gap continuity and confidence. Large masks with high continuity and high confidence are treated as high-risk alarms, while high-probability but low-reliability samples are remeasured or manually verified.

The output is also designed for later traceability. If the repeated warnings are due to edge uncertainty, then the camera or light-station should be checked. If the repeated warnings are due to bridge continuity, increase the quantity of solder, adjust the shape of the pad, or change reflow conditions. Therefore, the model will have both instant segmentation and extended-process diagnosis functions. This Design is suitable for high-mix PCB production because the product geometry can be altered, but the definition of bridging remains unchanged. Not all of the packages have the same pad pitch in the model. It uses the aligned pad-gap information to interpret the candidate region based on the local assembly structure.

4. Results and Discussion

4.1. Dataset Construction and Solder Bridging Morphology

A simulated dataset of 4,800 inspection windows for normal solder joints, weak bridge cases, severe bridge cases, paste-overflow cases and reflection artefacts has been generated. Figure 3 presents the dataset and defect morphology overview. As shown in Figure 3(a), normal samples are more frequent than bridging samples. Figure 3(b) shows weak bridges with very thin pad-gap connections, Figure 3(c) shows severe bridge examples, and Figure 3(d) shows pseudo-defect artefacts caused by glare and flux residue. Dataset construction studies [18] show that difficult negative samples are necessary for realistic industrial segmentation because ordinary background regions cannot test false-alarm control.

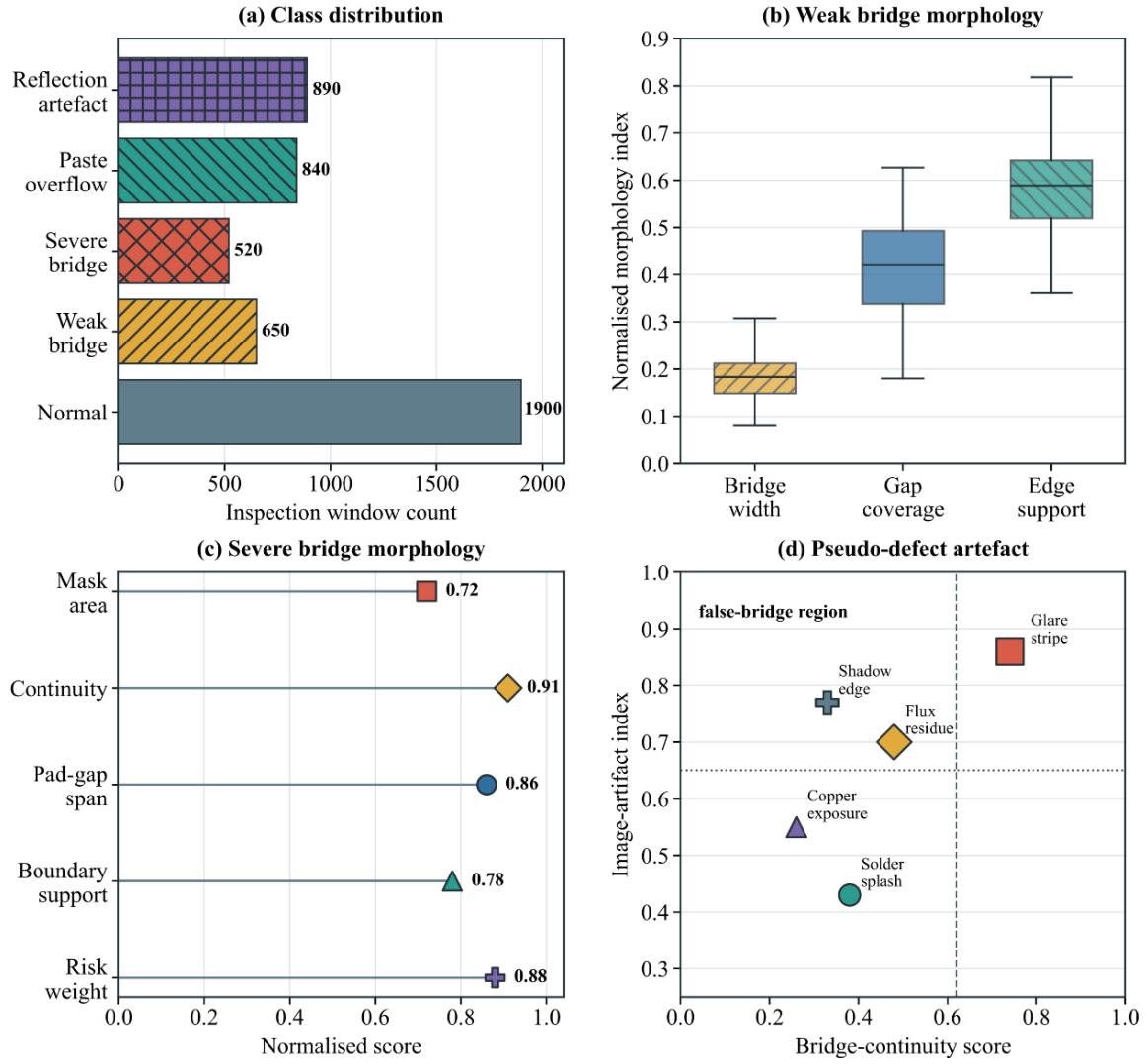


Figure 3. Dataset and solder bridging morphology overview. (a) Class distribution. (b) Weak bridge examples. (c) Severe bridge examples. (d) Pseudo-defect artefacts.

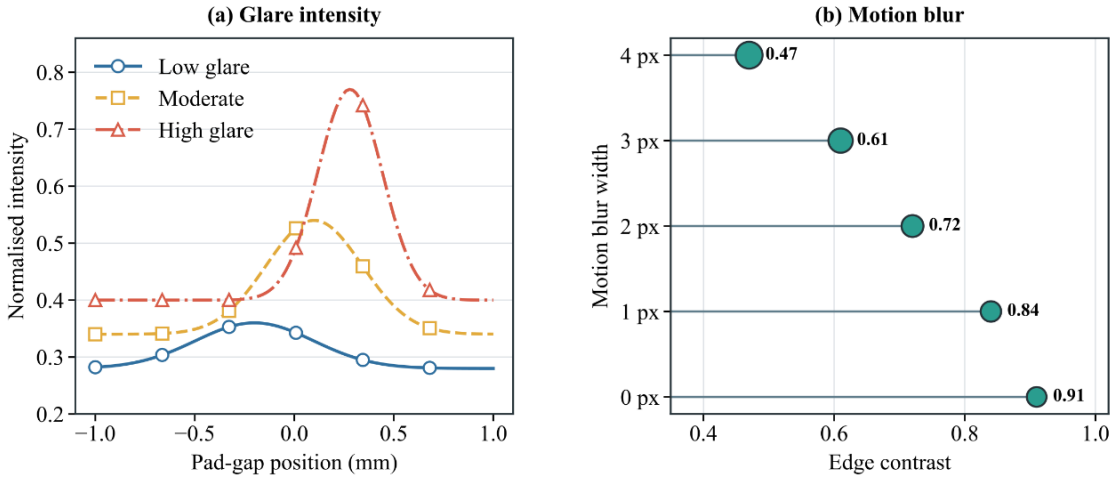


Figure 4. Image-quality disturbance conditions. (a) Glare intensity. (b) Motion blur.

The shape of solder bridges varies substantially. Some bridges are narrow and line-shaped, whereas others are wide paste connections between pins. Research on production defects [19] has shown that solder shape is affected by stencil printing, reflow profile and component pitch. The defective area is generally less than 2.5% of the inspection window, so high pixel accuracy alone may still miss a true bridge. Bridge recall, boundary F1 and review priority are therefore evaluated together. The segmentation result should represent a conductive path across pads, rather than a bright solder region without electrical continuity.

Figure 4 shows image-quality disturbance conditions. Figure 4(a) presents glare intensity near metallic pads, and Figure 4(b) shows blur caused by camera vibration or conveyor-speed fluctuation. Optical inspection research [20] has found that illumination instability is a common source of false alarms on reflective electronic assembly surfaces. In this dataset, glare, blur, shadow and partial occlusion are treated as reliability conditions rather than label errors. Glare may create a false bridge-shaped stripe, whereas blur may hide the boundary between two solder joints. The model therefore uses quality tags to adjust confidence and evidence weighting.

The two annotation types are bridge masks and edge-support labels. Boundary annotation is required to determine whether a predicted region overlaps the pad gap and therefore has bridge meaning. Benchmark studies of segmentation [21] have shown that boundary indicators are more sensitive to narrow defects than area indicators. A feasible production prediction must consider both bridge area and connection to nearby pads. When the predicted mask reaches both pad boundaries but remains thin, the sample is treated as a possible weak bridge; when the mask is large but lacks boundary support, it is treated as a false-positive candidate.

4.2. Segmentation Accuracy and Edge Robustness

Figure 5 shows segmentation results of various models. As shown in Figure 5(a), the proposed method achieves the highest mean intersection over union. Figure 5(b) shows that bridge recall improves most clearly for weak bridges. Figure 5(c) reports boundary F1, indicating that edge-aware representation improves pad-gap localisation. Figure 5(d) shows confidence reliability, where CausalTFT reduces overconfident false alarms. Segmentation research [22] has found that boundary-aware designs are particularly effective for small and thin industrial defects. The comparison indicates that solder bridging should be evaluated through mask overlap, boundary accuracy, bridge recall and confidence reliability together.

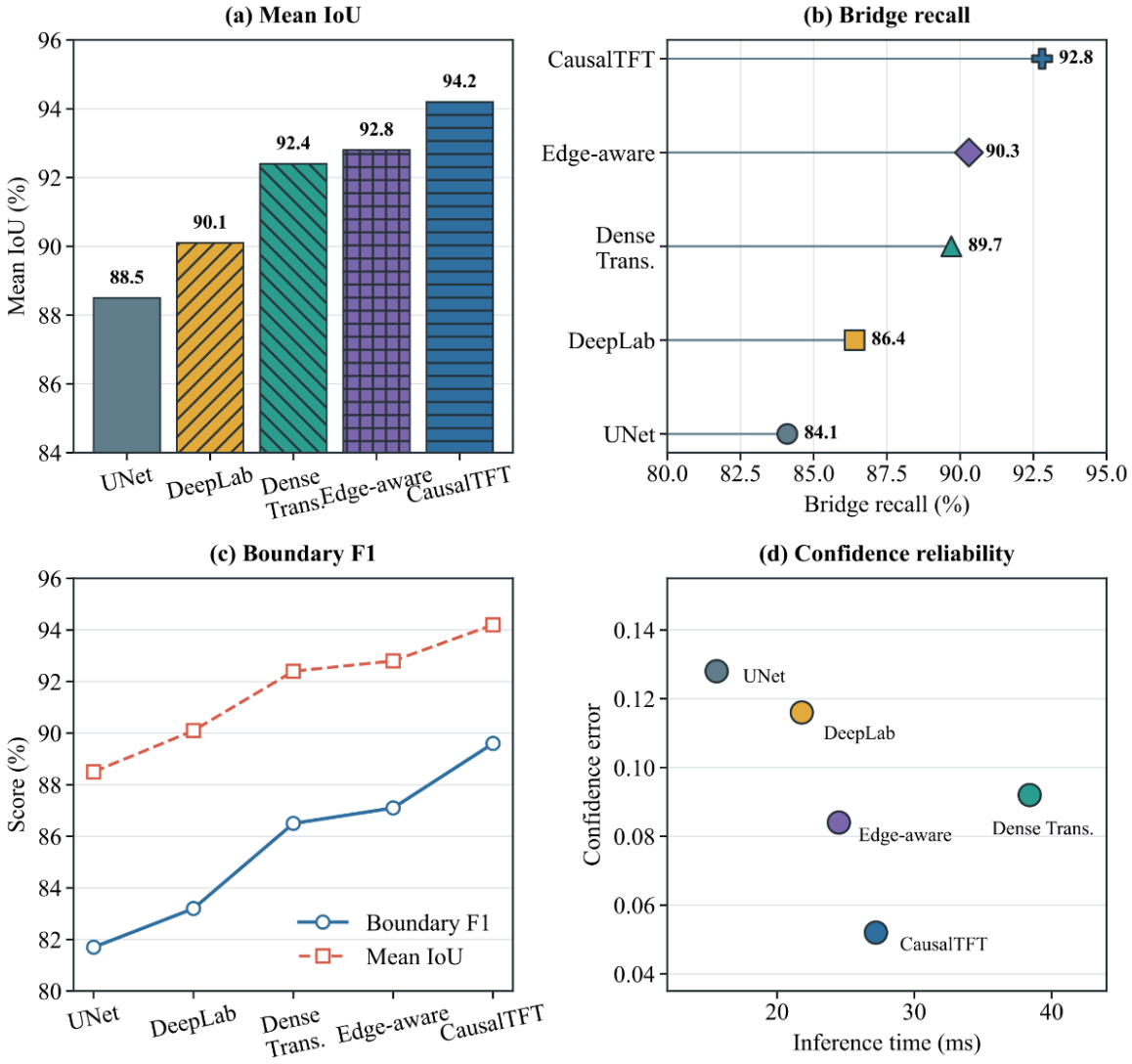


Figure 5. Segmentation performance comparison. (a) Mean IoU. (b) Bridge recall. (c) Boundary F1. (d) Confidence reliability.

Table 1 shows the actual data. Mean Intersection over Union (mIoU) is 0.942%, bridge recall is 0.928%, and boundary F1 is 0.896%. Dense Transformer baseline has improved the global context, but it is relatively slow in inference. The original UNet has a problem of poor boundary stability. Efficient inspection studies [23] require balancing the accuracy and speed of line-side systems. The proposed model still meets the requirements for the simulated production, and sparse evidence and causal gating reduce the amount of computation in the stable background area. Inference speed is required for a high-throughput inspection station of many boards. Although it is not the fastest among the options, the proposed model can meet the demands for simulated line-side speed. The extra cost will help to improve the recall of weak-bridge and confidence reliability. A relatively fast model that cannot detect some rare bridge cases is not suitable for quality control.

Table 1. Segmentation accuracy and inference speed comparison.

Model	Mean IoU (%)	Bridge Recall (%)	Boundary F1 (%)	Time (ms)
UNet	88.5	84.1	81.7	15.6
DeepLab-Style	90.1	86.4	83.2	21.8
Dense Transformer	92.4	89.7	86.5	38.4
Edge-Aware Baseline	92.8	90.3	87.1	24.5
CausalTFT	94.2	92.8	89.6	27.2

Ablation experiments show the function of each module. Removing edge-aware representation reduces boundary F1 because the model becomes less sensitive to pad-gap geometry. Removing causal gating increases false alarms under glare, and removing confidence calibration weakens review ranking. Ablation studies in industrial vision [24] have shown that deployment-related indicators should be used in addition to general accuracy. The current ablation analysis therefore considers recall, false alarms, boundary quality and confidence. Calibration separates suspicious samples from obvious defects and improves allocation of review resources.

Figure 6 shows edge robustness under disturbance. Figure 6(a) shows bridge recall under increasing glare, and Figure 6(b) shows boundary F1 under additional blur. Robust inspection research [25] shows that controlled disturbance tests prevent clean-image performance from being overestimated. In the proposed model, poor image quality lowers confidence and routes unstable masks to manual inspection rather than automatic acceptance. The disturbance test keeps the defect mask unchanged while modifying glare and blur, which helps determine whether the model responds to true defect geometry or imaging artefacts.

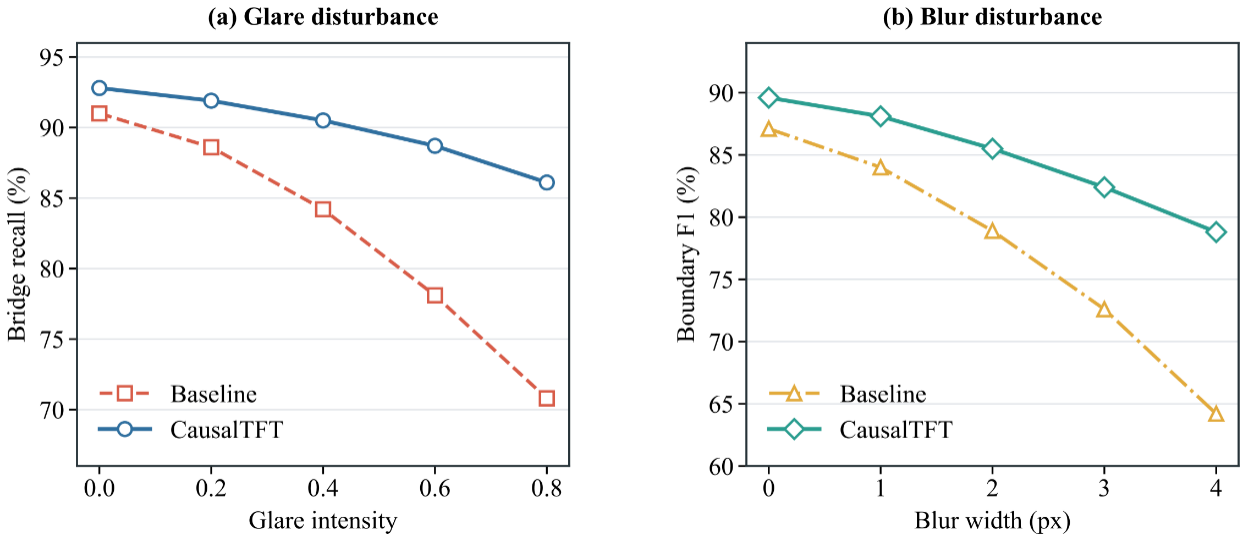


Figure 6. Edge robustness under disturbance. (a) Glare disturbance. (b) Blur disturbance.

Three error-analysis categories are observed. The first is a narrow true bridge partly obscured by component shadow. The second is a reflection stripe in the pad gap without an actual solder joint. The third is a solder splash near one pad that appears bridge-like but is not connected to the adjacent pad. Reliability studies of inspections [26] indicate that a failure taxonomy is useful because the same accuracy score may have different process causes. Evidence output helps distinguish edge discontinuity, brightness response and image-quality degradation, which correspond to different engineering responses.

4.3. Causal Evidence and Production Review Output

Figure 7 shows causal evidence and production review output. Figure 7(a) shows the leading evidence for accepting normal samples, where stable pad-edge separation is the primary reason. Figure 7(b) shows ranked evidence for a true bridge alarm, where edge continuity and solder-region connection dominate. Figure 7(c) reports low-confidence causes from glare or blur, and Figure 7(d) presents review-priority categories in the production system. Explainable industrial AI studies [27] have shown that evidence-level output increases engineering trust by linking model alarms with inspection actions. The explanation is therefore an auditable production signal rather than a decorative heatmap.

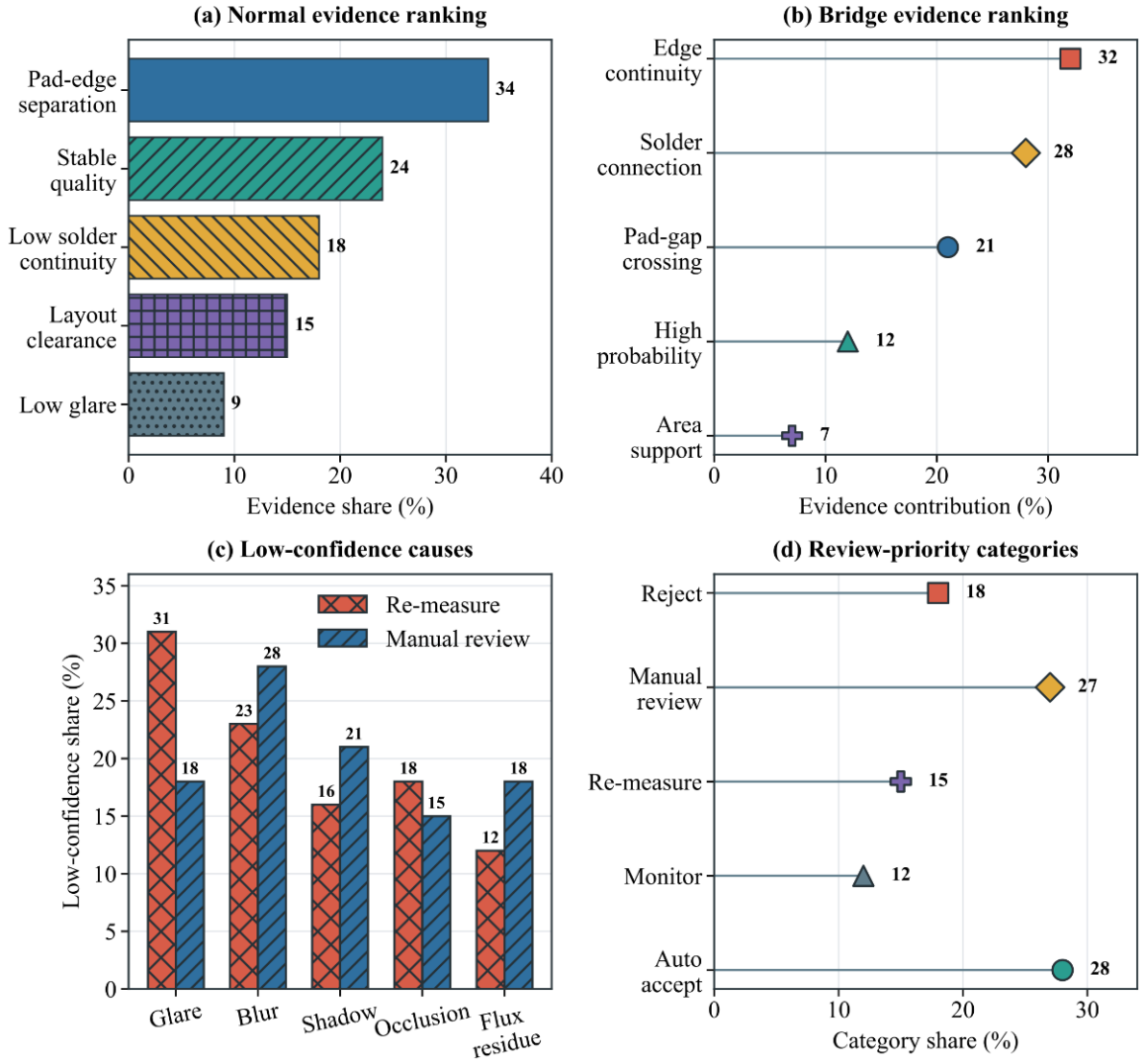


Figure 7. Causal evidence and production review output. (a) Normal evidence ranking. (b) Bridge evidence ranking. (c) Low-confidence causes. (d) Review-priority categories.

The confidence score should be interpreted together with the predicted bridge mask. High bridge probability with high confidence supports rejection or repair, while high probability with low confidence should trigger secondary review. Research on quality management [28] indicates that inspection decisions should account for measurement uncertainty. Production review records can also diagnose process problems: repeated alarms caused by edge discontinuity near the same package type may require stencil, paste-volume or placement-offset review, whereas repeated glare-related alarms may require imaging-station adjustment. Research on manufacturing analytics [29] links defect alarms with process context to identify recurring causes.

False alarms are not entirely eliminated. Some bright flux patterns still resemble narrow bridges in local shadow, and some weak bridges are partly hidden by component edges. Robust segmentation studies [30] have shown that uncertain samples should be sent for reassessment rather than forced into a binary decision. Serious bridges are infrequent but expensive, while normal joints are common in daily production. Cost-sensitive inspection studies [31] warn against ignoring high-risk defects for overall accuracy. The review-priority output organizes alarms by risk and reliability so that weak bridges are not suppressed and reviewers are not overloaded by low-value warnings.

Only a simulated dataset is available for this study. Real PCB lines may include more component packages, solder-mask colours, surface finishes and camera modules. Transfer evaluation studies [32] suggest that industrial models should be tested across product families before deployment. Future validation should acquire field images from multiple board types and inspection stations. Long-term drift in paste printing, stencil wear and reflow temperature may gradually alter defect appearance, and predictive quality-control research [33] shows that inspection models require recalibration when process distributions change. Confidence statistics and review results should therefore be tracked over time.

The proposed output can be connected with production databases. Alarm records should be linked with component type, board lot, inspection station and repair status. Traceable Quality Systems [34] require this connection to support immediate rejection and root-cause analysis. Research on industrial deployment [35] indicates that models are more effective when results can be audited and linked to actions. The mask, confidence and dominant evidence can help engineers determine whether an alarm originates from solder discontinuity, image abnormality or process drift. Confirmed false alarms and missed bridges can then guide data collection, camera recalibration or process adjustment.

5. Conclusion

This study developed an edge-aware CausalTFT model for PCB solder bridging segmentation, and the overall conclusion is that solder-region response, pad-edge support, bridge continuity, image-quality reliability and review-oriented outputs should be evaluated jointly for traceable assembly inspection. First, the simulated results show a mean intersection over union of 94.2%, bridge recall of 92.8% and boundary F1 of 89.6%, indicating that edge-aware representation and causal gating improve weak-bridge detection and boundary localisation. Second, the comparative results show that the proposed model outperforms UNet, DeepLab-style, dense Transformer and edge-aware baselines while retaining a practical inference time of 27.2 ms. Third, the main limitation is that the evaluation uses simulated data and simplified product variations; therefore, future validation should include field images across board types, package pitches, solder-mask colours, inspection stations, electrical-test outcomes and repair histories.

The proposed output separates bridge mask, bridge probability, confidence, dominant evidence and review priority. This structure supports rejection or repair for high-confidence conductive bridges, secondary review for low-confidence candidates and station calibration when repeated alarms are caused by glare, blur or weak boundary evidence. It also helps process engineers distinguish stencil-aperture, paste-volume, placement-offset and imaging-condition issues.

Future work should acquire real production images covering additional board types, package pitches, solder-mask colours, surface finishes and inspection stations. The model should also be connected to electrical test data, repair history and closed-loop review records to confirm whether predicted bridge masks correspond to actual circuit risk. Multi-camera or multi-illumination inspection should be evaluated for fine-pitch packages, because the same board region may reveal different evidence under different viewing conditions. These extensions will support safer and more traceable deployment in complex PCB assembly environments.

6. Declarations

6.1. Author Contributions

Poyraz Korkmaz contributes to conceptualization, methodology, software, validation, analysis, investigation, data collection, draft preparation, manuscript editing, visualization, supervision, project administration, and funding acquisition. Davut Gür contributes to validation, analysis, investigation, data collection, draft preparation. Farkas Tamás contributes to conceptualization, validation, analysis. All authors have read and agreed with the manuscript before its submission and publication.

6.2. Funding and Acknowledgments

This research received no specific financial support from any funding agency.

6.3. Institutional Review Board Statement

Not applicable.

6.4. Informed Consent Statement

Not applicable.

6.5. Data Availability

Not applicable.

6.6. Declaration of Competing Interest

The authors declare that they have no known competing financial interests or personal relationships that could have appeared to influence the work reported in this paper.

6.7. Declaration of generative AI and AI-assisted technologies

During the preparation of this manuscript, the authors utilized Grammarly for linguistic polishing, logical organization and draft revision. The generative AI tool was not involved in research design, data collection, data analysis, or the equation of core conclusions. All outputs generated by AI were reviewed, revised and verified manually by the authors. The authors take full responsibility for all content of this manuscript.

7. References

[1] Chen, K., Zhang, Y., Cheng, G., & Zhang, Y. (2024). A machine learning and finite element simulation-based void inspection for higher solder joint reliability. Microelectronics Reliability, 154, 115323. https://doi.org/10.1016/j.microrel.2024.115323

[2] Petkov, N., & Ivanova, M. (2024). Printed circuit board and printed circuit board assembly methods for testing and visual inspection: A review. Bulletin of Electrical Engineering and Informatics, 13(4), 2566–2585. https://doi.org/10.11591/eei.v13i4.7601

[3] Guo, H., Zhao, H., Zhao, Y., & Liu, W. (2024). PCB defect detection algorithm based on deep learning. Optik, 315, 172036. https://doi.org/10.1016/j.ijleo.2024.172036

[4] Guo, Q., Chen, Y., Zhu, Y., & Chen, D. (2025). CM-UNetv2: An enhanced semantic segmentation model for precise PCB defect detection and boundary restoration. Sensors, 25(16), 4919. https://doi.org/10.3390/s25164919

[5] Liu, Z., & Notni, G. (2025). A lightweight investigation on automated visual SMD-PCB inspection based on multimodal one-class novelty detection. Measurement: Sensors, 38, 101825. https://doi.org/10.1016/j.measen.2025.101825

[6] Chen, W., Wang, Z., & Zhao, H. (2024). PCB plug-in solder joint defect detection method based on coordinated attention-guided information fusion. Scientific Reports, 14(1), 19864. https://doi.org/10.1038/s41598-024-70100-7

[7] Li, Y., Ma, Z., & Ma, R. (2026). Efficient dual-branch high-resolution transformer design for crack segmentation. Applied Soft Computing, 189, 114513. https://doi.org/10.1016/j.asoc.2025.114513

[8] Rožanec, J. M., Šircelj, B., Fortuna, B., & Mladenić, D. (2024). Adaptive explainable artificial intelligence for visual defect inspection. Procedia Computer Science, 232, 3034–3043. https://doi.org/10.1016/j.procs.2024.02.119

[9] Cao, N., Farrag, A., Won, D., & Yoon, S. W. (2024). XSCAN: Explainable solder joint defect probability prediction through solder pastes printing status with imbalanced data. Journal of Manufacturing Systems, 77, 212–227. https://doi.org/10.1016/j.jmsy.2024.09.009

[10] Pal, P. K., Kataria, B., & Jangid, J. (2026). Schematic-aware PCB inspection using computer vision and deep learning for trace, solder, and net-level fault detection. IEEE Transactions on Components, Packaging and Manufacturing Technology, 16(6), 1423–1439. https://doi.org/10.1109/tcpmt.2026.3687148

[11] Elleuch, J. F., Mehdi, M. Z., Kammoun, H. M., Bellaaj, M., & Sellami, D. (2024). New possibilistic formalism based on confidence levels for metallic surface defect classification. IEEE Access, 12, 93010–93019. https://doi.org/10.1109/access.2024.3414840

[12] Qiu, S., Chen, J., Zhang, H., Wan, R., Xue, X., & Pu, J. (2024). Guided contrastive boundary learning for semantic segmentation. Pattern Recognition, 155, 110723. https://doi.org/10.1016/j.patcog.2024.110723

[13] Zhong, X., & Sun, Z. (2026). Boundary-local soft supervision for reliable calibration in defect segmentation. IEEE Signal Processing Letters, 33, 3791–3795. https://doi.org/10.1109/lsp.2026.3731530

[14] Tang, H., Chen, S., Liu, Y., Wang, S., Chen, Z., & Hu, X. (2024). Boundary-aware dichotomous image segmentation. The Visual Computer, 40(12), 9051–9062. https://doi.org/10.1007/s00371-024-03295-5

[15] Zhou, X., Ye, W., Xie, R., & Zhang, S. (2025). Mitigating spurious correlations with causal logit perturbation. Information Sciences, 717, 122276. https://doi.org/10.1016/j.ins.2025.122276

[16] Yan, L., & Xiao, J. (2026). Temporal-variable Transformer with adaptive cross-stream gated fusion for multivariate time series classification. IEEE Access, 14, 120920–120934. https://doi.org/10.1109/access.2026.3719357

[17] Bitterling, C., Loske, D., & Klumpp, M. (2025). Improving visual inspection accuracy: Explainable AI for human-centric quality control. IFAC-PapersOnLine, 59(10), 1450–1455. https://doi.org/10.1016/j.ifacol.2025.09.244

[18] Bai, D., Li, G., Jiang, D., Yun, J., Tao, B., Jiang, G., et al. (2024). Surface defect detection methods for industrial products with imbalanced samples: A review of progress in the 2020s. Engineering Applications of Artificial Intelligence, 130, 107697. https://doi.org/10.1016/j.engappai.2023.107697

[19] Alakayleh, A., Hamasha, S., & Alahmer, A. (2024). The impact of paste alloy, paste volume, and surface finish on solder joint. Microelectronics Reliability, 160, 115457. https://doi.org/10.1016/j.microrel.2024.115457

[20] Weiss, E. (2024). Advancements in electronic component assembly: Real-time AI-driven inspection techniques. Electronics, 13(18), 3707. https://doi.org/10.3390/electronics13183707

[21] Ma, R., Li, C., Xing, Y., Wang, S., Ma, R., Feng, F., et al. (2025). Defect focused Harris3D and boundary fine-tuning optimized region growing: Lithium battery pole piece defect segmentation. Measurement, 242, 116147. https://doi.org/10.1016/j.measurement.2024.116147

[22] Rezvani, S., Fateh, M., & Khosravi, H. (2024). ABANet: Attention boundary-aware network for image segmentation. Expert Systems, 41(9), e13625. https://doi.org/10.1111/exsy.13625

[23] Ashourpour, M., & Azizpour, G. (2025). Edge-deployed deep learning for automated quality control in industrial assembly: A case study in real-time defect detection. Procedia CIRP, 134, 735–740. https://doi.org/10.1016/j.procir.2025.02.180

[24] Wang, C., Wei, X., & Jiang, X. (2024). An automated defect detection method for optimizing industrial quality inspection. Engineering Applications of Artificial Intelligence, 127, 107387. https://doi.org/10.1016/j.engappai.2023.107387

[25] Lara, M. A., Hameed, I. A., & Koziorek, J. (2025). Anomaly-focused augmentation method for industrial visual inspection. IEEE Access, 13, 89118–89139. https://doi.org/10.1109/access.2025.3570075

[26] Pant, H., & Singh, S. B. (2024). Multi-objective inspection optimization of periodically inspected multi-failure mode system. International Journal of Reliability, Quality and Safety Engineering, 31(2), 2450003. https://doi.org/10.1142/s0218539324500037

[27] Oliveira, R. M. A., Sant'Anna, Â. M. O., & da Silva, P. H. F. (2024). Explainable machine learning models for defects detection in industrial processes. Computers & Industrial Engineering, 192, 110214. https://doi.org/10.1016/j.cie.2024.110214

[28] Kolus, A., & Duffuaa, S. O. (2025). Determining optimal process means in a multi-stage production system with inspection errors in 100% inspection. Quality Technology & Quantitative Management, 22(1), 105–130. https://doi.org/10.1080/16843703.2024.2312016

[29] Zhang, C., Dong, J., Peng, K., & Zhang, H. (2024). Spatio-temporal information analytics-based performance-driven industrial process monitoring framework with cloud-edge-device collaboration. Journal of Manufacturing Processes, 110, 224–237. https://doi.org/10.1016/j.jmapro.2023.12.036

[30] Vijayakumar, A., Koilraj, J. A. S., & Rajappa, M. (2025). PharmaNet Deep: Real-time pharmaceutical defect detection using defect-guided feature fusion and uncertainty-driven inspection. International Journal of Computational Intelligence Systems, 18(1), 250. https://doi.org/10.1007/s44196-025-00986-2

[31] Lario, J., Mateos, J., Psarommatis, F., & Ortiz, Á. (2026). A cost model for the investment feasibility of quality inspection technologies in the Zero-Defect Manufacturing era. International Journal of Production Research, 64(17), 7359–7374. https://doi.org/10.1080/00207543.2024.2383780

[32] Lee, S. J. (2025). Few-shot adaptation of foundation vision models for PCB defect inspection. Journal of Imaging, 11(11), 415. https://doi.org/10.3390/jimaging11110415

[33] Lončarević, Z., Reberšek, S., Šela, S., Skvarč, J., Ude, A., & Gams, A. (2024). Adaptive visual quality inspection based on defect prediction from production parameters. IEEE Access, 12, 93899–93910. https://doi.org/10.1109/access.2024.3424664

[34] Wang, K., Liu, C., & Lu, Y. (2024). Ensemble Bayesian Network for root cause analysis of product defects via learning from historical production data. Journal of Manufacturing Systems, 75, 102–115. https://doi.org/10.1016/j.jmsy.2024.06.001

[35] Jayawardena, A., Sul, J. H., Moratuwage, D., Wijayaraja, J. L., & Piyathilaka, L. (2026). State of the art in AI-based visual inspection for industrial quality control: Methods, benchmarks, challenges, and autonomous systems. Electronics, 15(12), 2727. https://doi.org/10.3390/electronics15122727